Peer-reviewed version available at *Nature Communications* **2019**; doi:10.1038/s41467-019-08835-5

High performance n-type Ag_2Se film on nylon membrane for flexible thermoelectric power generator

Yufei Ding[1], Yang Qiu[2], Kefeng Cai[1*], Qin Yao[3], Song Chen[4], Lidong Chen[3*], Jiaqing He[2*]

1. Key Laboratory of Advanced Civil Engineering Materials, Ministry of Education, School of Materials Science & Engineering, Tongji University, 4800 Caoan Road, Shanghai 201804, China

2. Physics department, Southern university of Science and Technology, 1088 XueYuan Avenue, Shenzhen 518055, China

3. State Key Laboratory of High Performance Ceramics and Superfine Microstructure, Shanghai Institute of Ceramics, Chinese Academy of Science, Shanghai, 200050, China

4. School of Materials Science and Engineering, Fujian University of Technology, Fuzhou 350108, China

***Corresponding author**: kfcai@tongji.edu.cn； he.jq@sustc.edu.cn; cld@mail.sic.ac.cn

Abstract

Researches on flexible thermoelectric (TE) materials usually focus on conducting polymers (CPs) and CP-based composites; however, it is a great challenge to obtain high TE properties comparable to inorganic counterparts. Here, we report an n-type Ag_2Se film on flexible nylon membrane with an ultrahigh power factor ~ 987.4 ± 104.1 $\mu Wm^{-1}K^{-2}$ at 300 K and an excellent flexibility (93% of the original electrical conductivity retention after 1000 bending cycles around a 8-mm diameter rod). The flexibility is attributed to a synergetic effect of the nylon membrane and the Ag_2Se film intertwined with numerous high-aspect-ratio Ag_2Se grains. A TE prototype composed of 4-leg of the hybrid film generates a voltage and a maximum power of 19 mV and 460 nW, respectively, at a temperature difference of 30 K. This work opens opportunities of searching for high performance TE film for flexible TE devices.

Key words: thermoelectric, flexible, n-type, Ag_2Se, hot-pressing

Introduction

Nowadays, the explosive growth of wearable devices has stimulated the development of materials which can power the devices with the energy harvesting from the human body[1]. Flexible thermoelectric (TE) materials as the promising energy-harvesting materials, which can directly convert heat into electricity or vice versa and realize the self-power for wearable devices from the temperature difference between the skin and the ambient environment, have attracted increasing attention[1–8]. The TE performance of a materials is evaluated by the dimensionless figure of merit, $ZT = \alpha^2\sigma T/\kappa$, where α, σ, and κ are the Seebeck coefficient, electrical conductivity, and thermal conductivity of the material, respectively, and T is the absolute temperature.

Until now, the research on flexible TE materials mainly focuses on conducting polymers (CPs) and CP-based composite materials [9–12]; although much progress has been made[4,13–15], their ZT values are still incompatible to those of the inorganic TE materials. Moreover, the CP-related materials are mainly p-type ones while their n-type counterpart is still lacking. For the completion of a high efficiency flexible TE module, high performance of n-type materials are very desirable.

Besides the CPs, insulating polymers are also employed for forming TE composites with inorganic TE materials. For example, most recently, Hou et al.[16] prepared p-type $Bi_{0.5}Sb_{1.5}Te_3$ and epoxy resin composite thick film by hot-pressing (623 K, 4 MPa) and the film shows a high power factor ($\alpha^2\sigma$) of 840 $\mu W\ m^{-1}\ K^{-2}$. Recently, flexible substrate, such as polyimide, fiber or paper, has been used to support inorganic materials for preparing high performance and flexible TE materials[17–22]. For instance, Gao et al.[20] reported a novel glass-fiber-aided cold-pressing method for flexible n-type Ag_2Te films on copy paper and the power factor value was up to 85 $\mu W\ m^{-1}\ K^{-2}$ at 300 K. Choi et al.[21] prepared n-type HgSe nanocrystal thin film by spin-coating HgSe nanocrystal solution on a plastic substrate and the film showing a maximum power factor of 550 $\mu W\ m^{-1}\ K^{-2}$ at 300K. Jin et al.[22] deposited Bi_2Te_3 thick film on a cellulose fibers paper via an unbalanced magnetron sputtering technique and the composite film exhibits good flexibility and a power factor of ~250 $\mu W\ m^{-1}\ K^{-2}$ at room temperature.

β-Ag_2Se is a narrow band semiconductor with an energy gap E_g=0.07 eV at 0 K and it transforms into a cubic superionic conductor (α-Ag_2Se) around 407 K. β-Ag_2Se, which exhibits high electrical conductivity and low thermal conductivity, has the great potential for n-type TE material near room temperature. Several groups have

reported the TE performance of Ag_2Se[23–25]. For instance, Ferhat et al.[26] prepared β-Ag_2Se bulks by a direct-reaction of the element Ag and Se in evacuated quartz tubes at 1273 K and the maximum power factor of the material was about 3500 μW m^{-1} K^{-2}, which is similar to that of the state-of-art material at room temperature. Most recently, Perez-Taborda et al.[27] deposited Ag_2Se films on glass substrates via pulsed hybrid reactive magnetron sputtering and the films showing a high power factor ~ 2440 μW$m^{-1}K^{-2}$ at room temperature. Nevertheless, the films are with relatively high cost since an expensive facility is used.

Although Ag_2Se materials with excellent TE performance at room temperature have been reported, they are all non-flexible. In this work, we developed a facile strategy to prepare n-type flexible Ag_2Se film on a nylon membrane. The hybrid film showed a very high power factor of 987.4 μW$m^{-1}K^{-2}$ at 300 K, which is one of the best values reported for flexible n-type materials and even comparable to that of some high-ZT inorganic bulk materials at high temperatures, such as SnSe (~900 μW$m^{-1}K^{-2}$ at 773 K)[28] and $Cu_{2-x}Se$ (1200 μW$m^{-1}K^{-2}$ at 1000 K)[29].

Methods

Synthesis. The Ag_2Se film was prepared by a vacuum-assisted filtration of a Ag_2Se-nanowire dispersion on a porous nylon membrane and the film on the nylon membrane was dried at 60 ºC in vacuum overnight and then hot-pressed at 200 ºC and 1 MPa for 30 min. See details in supplementary Figs. 1-3.

Characterization. The phase composition of the Ag_2Se film was examined by X-ray diffraction (XRD) using Cu Kα radiation (D /MAX 2550VB3 + /PC Ⅱ). The morphology of the film was observed by a field emission scanning electron microscope (FESEM, FEI Nova NanoSEM 450). The internal microstructure of the film was examined by double-aberration corrected transmission electron microscope (TEM, FEI Titan @300kV in TEM and STEM mode), and the TEM sample was prepared by the Focused Ion Beam (FIB, FEI Helios600i) with the in-situ lift-out technique. To protect the sample surface before the ion milling, a Pt layer was sputtered on the full sample. The region of interest was further locally capped in the FIB with ion beam deposited carbon. The major milling was done with a 30 kV Ga ion beam while the milling progress was controlled with the scanning electron microscope. Final milling to minimize the damage layer on the specimen was performed with 5 kV followed by 2 kV Ga ion beam.

Measurement of TE properties and performance. The in-plane electrical conductivity and Seebeck coefficient were measured by the standard four-probe method (Sinkuriko, ZEM-3) in He atmosphere. The measurement error for σ and α is about ±5%. The thickness of the films was determined by a thickness meter (Shanghai Liu Ling Instrument Factory) combined with FESEM observation. The bending test of the film was performed using a homemade apparatus around a rod with a diameter of 8 mm.

The film was cut into strips (20 mm × 5 mm), and the strips were pasted on a polyimide substrate (the interval of two strips is ~5 mm). The two ends of each strip were coat with a layer of Au via a mask and evaporation. After that, each strip was connected in series with Ag paste as conductive connection to obtain a prototype power generator. The output voltage and output power of the device were measured by a homemade apparatus (see supplementary Fig. 6).

Results

Characterization of Ag_2Se film. XRD analysis of the film reveals that all the XRD peaks (Fig.1a) can be indexed to β-Ag_2Se phase (JCPDS No. 24-1041). The XRD peaks for the Ag_2Se film are stronger than those for the Ag_2Se nanowires (NWs) (supplementary Fig. 3), and especially the (002) and (004) plane peaks become particularly strong, indicating increase of crystallinity and a large number of the Ag_2Se grains preferentially grown along the (*00l*) plane[30]. The thickness of the Ag_2Se film is about 10 μm (supplementary Fig. 5).

After hot pressing, the Ag_2Se NWs with diameter of ~65 nm and length of a few microns are sintered into a network-like film with numerous submicron pores (Fig. 1(b)(c)). Although the hot pressing temperature (200 ^oC) is much lower than the melting point (880 ^oC) of Ag_2Se, the film is relatively dense due to highly active Ag_2Se NWs.

To investigate more detailed microstructure of the film, transmission electron microscope (TEM) sample was prepared by FIB and studied by high-angle annular dark field scanning TEM (HADDF-STEM). Fig. 1(d) shows an overview HADDF-STEM image. Although pores ranging from dozens of nanometers to several-hundred nanometers and microgaps indicated by arrows can be observed, generally interior of the film is also dense. Fig. 1(e) shows a typical STEM image. The white dots in (e) are Pt introduced during the TEM sample preparation.

Fig. 1(f) is a FFT pattern corresponding to (e). Fig. 1(g) is a typical HRSTEM image, in which the dot-lines shows grain boundaries, showing well sintered of the Ag_2Se nanograins with different orientations and defects (edge dislocations and stacking faults).

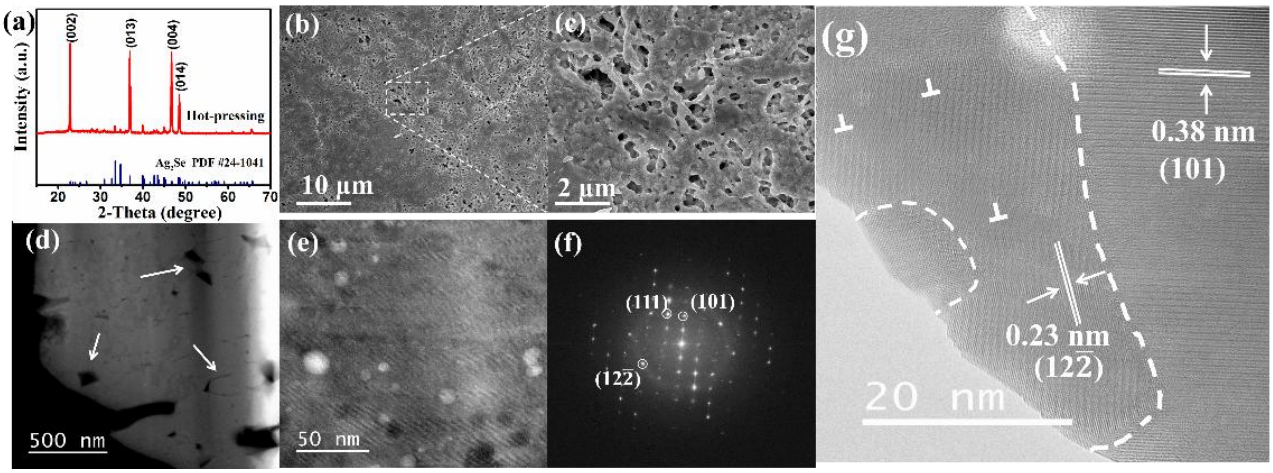

Figure 1 Characterization of the Ag_2Se film. (a) XRD pattern of the Ag_2Se film, (b) typical surface FESEM images of the Ag_2Se film at low (b) and high (c) magnification； (d) an overview HADDF-STEM image, (e) a typical STEM image, (f) a FFT image corresponding to (e), and (g) a typical HRSTEM image.

TE properties of the Ag_2Se film. Fig. 2 exhibits the TE properties of the Ag_2Se film from 300 to 453 K. The Seebeck coefficient of the film at 300 K is about -140.7 μV K^{-1}, indicating n-type conduction. As temperature increases, the absolute Seebeck coefficient shows a decrease tendency and it decreases rapidly when the temperature increases from 393 to 423 K. The electrical conductivity of the film is ~497 S/cm at 300 K and it increases with the temperature increasing from 300 to 393 K and also decreases rapidly when the temperature changes from 393 to 423 K. The change tendency of the Seebeck coefficient and electrical conductivity for the film is similar to that of the bulk Ag_2Se reported in ref. 23. This is because there is a phase transformation for Ag_2Se from a semiconductor to a superionic conductor at 407 K. However, the change tendency of the electrical conductivity of the film is not as that for the Ag_2Se film reported in ref. 27, which may be due to different orientation of the films resulted from different preparation processes.

As a result, as the temperature increases, the power factor ($\alpha^2\sigma$) value also shows a similar change tendency to that of electrical conductivity: increases from 987.4 at 300 K to 1448.1 μ$Wm^{-1}K^{-2}$ at 393K, then rapidly

decreases to 569.2 $\mu Wm^{-1}K^{-2}$ at ~423 K. The power factor value at 300 K is among the best n-type flexible TE materials.

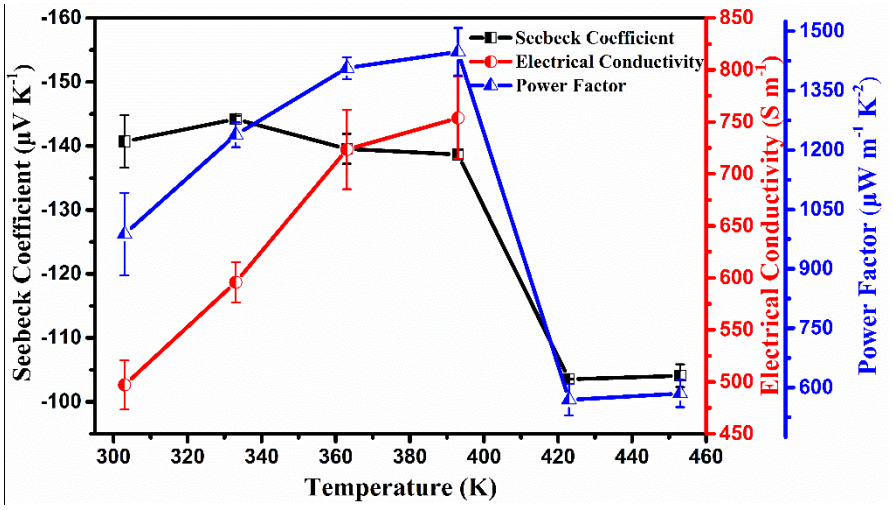

Figure 2 In-plane TE properties of the film. Temperature dependence of Seebeck coefficient, electrical conductivity and power factor for the Ag_2Se film.

Flexibility of the Ag_2Se film. In order to test the flexibility of the Ag_2Se film, a bending test was applied around a rod with a diameter of 8 mm. Fig.3(a) demonstrates the ratio (σ/σ_0) of the electrical conductivity with or without bending with different cycles. The electrical conductivity decreases slowly with the increasing of bending cycles. About 93% and 80% of the initial electrical conductivity are maintained after 1000 and 1500 bending cycles, respectively. This shows an excellent flexibility of the film.

In order to better understand the excellent flexibility of the film. We deliberately examined the details near the interface between the Ag_2Se film and the nylon membrane. We found that the Ag_2Se grains are well combined with the amorphous nylon membrane (Fig. 3(b)), indicating that there is a good bonding between them, resulted from the hot pressing, which is good for flexibility[20]. In Fig. 3(c), from left to right is a HAADF-STEM image near a heterointerface, overall corresponding EDS image, elemental EDS images of Ag, Se, C, N, and O, respectively. The elements of C, N, and O are attributed to the CONH group of the nylon. It is seen from the EDS images of elemental Ag and Se that a small amount of these two elements are detected in the nylon membrane. This is because the nylon membrane is porous (pore size ~ 200 nm), and some tips of the Ag_2Se nanowires may penetrate into the pores during the filtration and they bonded together during the hot pressing.

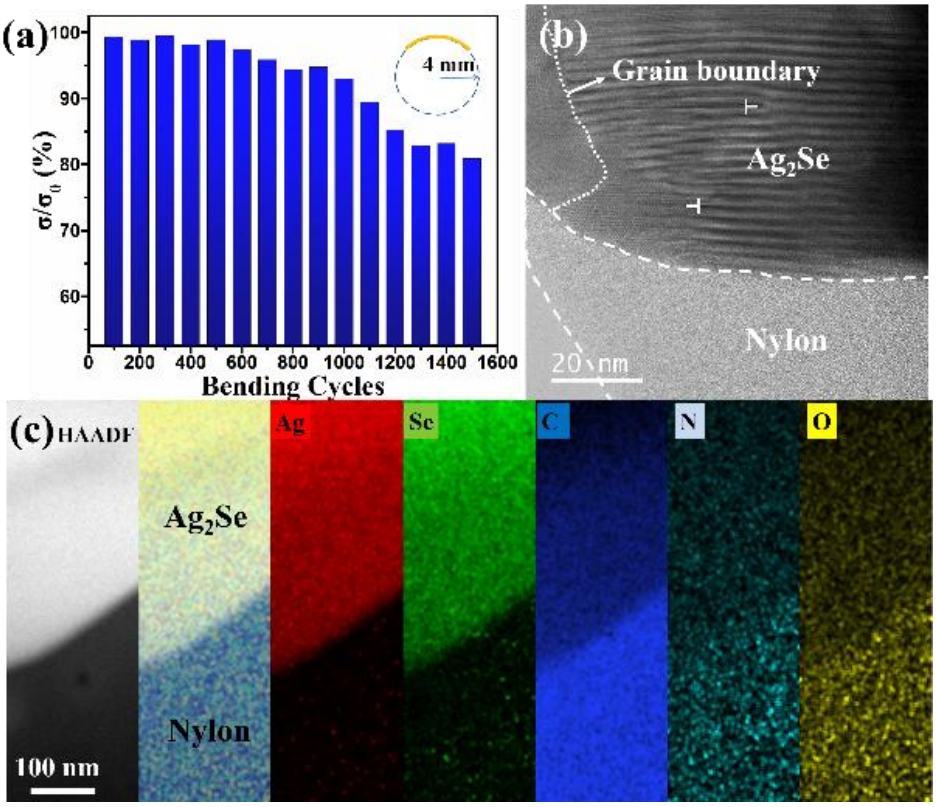

Figure 3 Flexibility of the film and evaluation of the heterointerface. (a) The ratio of electrical conductivity of the film before and after bending as a function of bending cycles, (b) A HRSTEM image showing good combination between Ag_2Se film and nylon membrane, (c) from left to right: a HAADF image of a heterointerface between a Ag_2Se grain (upper part) and nylon (lower part), overall corresponding EDS image and EDS image of elemental Ag, Se, C, N, and O

Therefore, the good flexibility of the hybrid film can be explained by the following reasons. (1) As known to all, nylon has an intrinsic excellent flexibility. (2) The Ag_2Se film is in fact a dense network intertwined with numerous Ag_2Se nanograins sintered from large aspect ratio of Ag_2Se nanowires; hence, the film itself should have a certain flexibility. (3) The nylon membrane and the Ag_2Se film have a good bonding (see Fig.3b, c). In addition, most recently, Shi et al. [31] reported that Ag_2S semiconductor exhibits an extraordinary metal-like ductility with high plastic deformation strains at room temperature. As Se and S are in the same family, Ag_2Se may have a similar ductility.

Device performance. As shown in Fig. 4, the TE prototype device consists of 4 pieces of the film. Each leg is 5 mm in width and 20 mm in length. To decrease the high electrical contact resistance between the film and

Preprints (www.preprints.org) | NOT PEER-REVIEWED | Posted: 13 September 2018 doi:10.20944/preprints201809.0229.v1

Peer-reviewed version available at Nature Communications 2019; doi:10.1038/s41467-019-08835-5

silver paste,[32,33] gold was first evaporated on two ends of each leg and then silver paste was painted to connect the legs in series. The open-circuit voltage and output power were measured with a homemade apparatus (see supplementary Fig.6). Fig. 4(a) shows the relationship between the open-circuit voltage and temperature difference. The open-circuit voltage is proportional to the temperature difference. When the temperature difference is 30 K, the open-circuit voltage is about 19 mV. When the load resistance equals to the inner resistance (R_{in}) of the device, the maximum output power is obtained. The output power (P) is calculated by the equation as follows:

$$P = \frac{U^2}{4R_{in}} = IU \qquad (1).$$

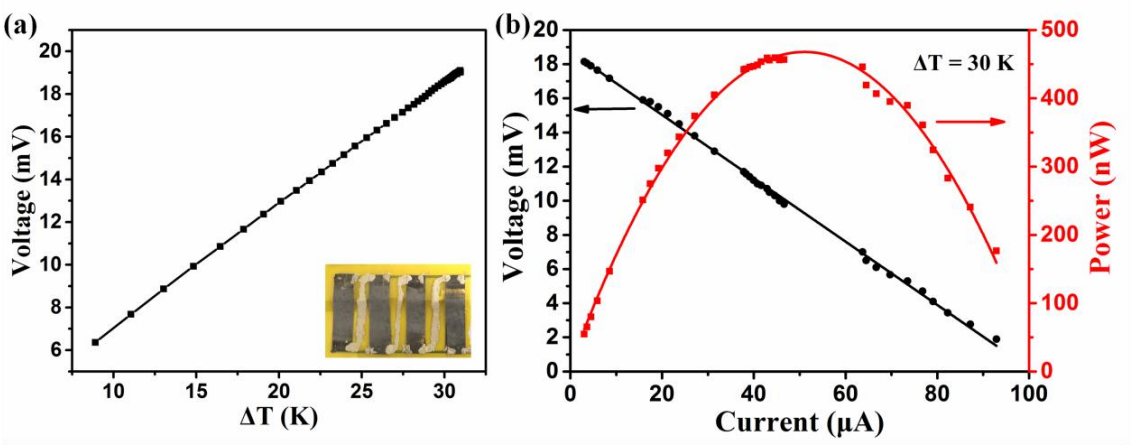

Fig. 4 Performance of the prepared device, (a) The open-circuit voltage at various temperature difference (inset is a digital photo of the TE prototype device), (b) The output voltage and output power versus current at temperature difference of 30 K.

The curve of output voltage - current and that of output power – current are shown in Fig. 4(b). The output voltage is inversely proportional to output current. At the temperature difference of 30 K, the maximum output power is about 460 nW. The maximum power density is about 2.3 W m^{-2}, obtained from dividing the power by the cross-sectional area and the number of legs[17], which is somewhat higher than that of reported flexible n-type devices[34–36], confirming that the hybrid film possesses high TE performance.

Table 1 Comparison of TE performance of flexible n-type TE materials at room temperature

Materials	α (μV K^{-1})	σ (S cm^{-1})	PF (μW m^{-1} K^{-2})	Ref.
Ag_2Te/copy-paper	-100	85	85	[20]
Cu-doped Bi_2Se_3/PVDF	-84	146	103.2	[37]
Ni NWs/PVDF	-20.6	4700	200	[38]
Bi_2Te_3/Cellulose fiber	-130	148	250	[22]
C_{60}/TiS_2	-101	390	400	[34]
HgSe	-518	20	550	[21]
TiS_2[tetrabutylammonium]$_{0.013}$ [hexylammonium]$_{0.019}$	-150	400	904	[39]
Ag_2Se/Nylon membrane	-140	497	987	This work

Discussion

In general, the thermal conductivity κ of a semiconductor consists of electronic κ_e and lattice contribution κ_l. As it is still a great challenge to measure the in-plane thermal conductivity of films[40], especially for the films with low thermal conductivity. In the present case, the hybrid film consists of the Ag_2Se film and nylon membrane, and both the components have intrinsic low thermal conductivity (bulk Ag_2Se ~0.6-1.0 W m^{-1} K^{-1} [23,25–27] and nylon ~0.25-0.36 W m^{-1} K^{-1} [41]), hence we could not provide the value. The Ag_2Se film grown by the pulsed hybrid reactive magnetron sputtering is with a $\kappa \sim 0.64 \pm 0.1$ W m^{-1} K^{-1}, in which κ_e~0.43 W m^{-1} K^{-1} calculated by $\kappa_e = L\sigma T$, assuming the Lorentz number L being 1.8×10^{-8} $W\Omega K^{-2}$ and κ_l~0.21 W m^{-1} K^{-1} [27]. In our case, a κ_e of 0.268 W m^{-1} K^{-1} is estimated by using the same Lorenz number. In addition, since our Ag_2Se film contains pores with sizes ranging from dozens of nanometers to a few hundred of nanometers, nanograins

(see Fig.1 (g)) and a hetero-interface between the Ag_2Se film and nylon membrane (see Fig.3b and supplementary Fig.5), the lattice contribution κ_l will be lower than that (κ_l~0.21 W m^{-1} K^{-1}) of the film consisting of Ag_2Se micrograins in ref. 27. This suggests that the in-plane thermal conductivity of our film will be lower than 0.478 W m^{-1} K^{-1}, which means that the ZT value of our film will be larger than 0.62 at 300 K.

The TE properties of a β-Ag_2Se single crystal from 160 to 300 K are calculated using the first-principle density functional theory (see details in supplementary Fig.7)[42]. The calculation shows that the power factor along the b-axis ((*0l0)* direction is about 2465 μW m^{-1} K^{-2} at 300 K, which is about two orders of magnitude higher than that along other two axes. Recall that the present film is preferentially grown along (*00l*) direction (see Fig.1(a)). This could be the main reason for our film showing lower power factor than that of the film (without preferential orientation) deposited on glass substrate by the pulsed hybrid reactive magnetron sputtering in ref. 27. This implies that the TE properties of our hybrid film can be further improved via tuning the orientation of the Ag_2Se grains.

In summary, we fabricated a high performance n-type flexible Ag_2Se/nylon hybrid film by a simple and facile method. A remarkable high power factor of 987.4±104.1 μW m^{-1} K^{-2} at 300 K was obtained, which is a record value among the recently reported n-type flexible TE materials (Table 1). The high power factor comes from the special Ag_2Se film; and the excellent flexibility of the hybrid film comes from the nylon membrane, the special Ag_2Se film, and good combination of the Ag_2Se film and nylon membrane. A prototype device with 4-leg of the film connected with silver paste was fabricated. The maximum power density of the prototype device is about 2.3 W m^{-2} at a temperature difference of 30 K. Together with the good TE properties of the Ag_2Se film and excellent flexibility of the nylon membrane, the hybrid film has shown great promise in flexible TE modules for wearable energy harvesting. This work demonstrates an effective route to fabricate high-performance flexible inorganic/organic hybrid TE films.

Data availability. The data that support the findings of this study are available from the corresponding author upon reasonable request.

References

1. Bahk, J., Fang, H. & Shakouri, A. Flexible thermoelectric materials and device optimization for wearable energy harvesting. *J. Mater. Chem. C* **3,** 10362–10374 (2015).
2. Bharti, M., Singh, A., Samanta, S. & Aswal, D. K. Progress in Materials Science Conductive polymers for thermoelectric power generation. *Prog. Mater. Sci.* **93,** 270–310 (2018).
3. Zhang, L. *et al.* Fiber-Based Thermoelectric Generators : Materials , Device Structures , Fabrication , Characterization , and Applications. *Adv. Energy Mater.* **8,** 1700524 (2017).
4. Park, T., Park, C., Kim, B., Shin, H. & Kim, E. Environmental Science power factors to generate electricity by the touch of fingertips. *Energy Environ. Sci.* **6,** 788–792 (2013).
5. Kim, S. J., We, J. H. & Cho, B. J. A wearable thermoelectric generator fabricated on a glass fabric. *Energy Environ. Sci.* **7,** 1959–1965 (2014).
6. Du, Y. *et al.* Thermoelectric Fabrics : Toward Power Generating Clothing. *Sci. Rep.* **5,** 6411 (2015).
7. Bae, E. J., Kang, Y. H., Jang, K. & Cho, S. Y. Enhancement of Thermoelectric Properties of PEDOT : PSS and Tellurium-PEDOT : PSS Hybrid Composites by Simple Chemical Treatment. *Sci. Rep.* **6,** 18805 (2016).
8. Song, H. & Cai, K. Preparation and properties of PEDOT:PSS/Te nanorod composite films for flexible thermoelectric power generator. *Energy* **125,** 519–525 (2017).
9. Snyder, G. J. & Toberer, E. S. Complex thermoelectric materials. *Nat. Mater.* **7,** 105–114 (2008).
10. Du, Y., Shen, S. Z., Cai, K. & Casey, P. S. Research progress on polymer – inorganic thermoelectric nanocomposite materials. *Prog. Polym. Sci.* **37,** 820–841 (2012).
11. Zhang, Q., Sun, Y., Xu, W. & Zhu, D. Organic Thermoelectric Materials : Emerging Green Energy Materials Converting Heat to Electricity Directly and Efficiently. *Adv. Mater.* **26,** 6829–6851 (2014).
12. Gayner, C. & Kar, K. K. Progress in Materials Science Recent advances in thermoelectric materials. *Prog. Mater. Sci.* **83,** 330–382 (2016).
13. Bubnova, O. *et al.* Optimization of the thermoelectric figure of merit in the conducting polymer poly(3,4-ethylenedioxythiophene). *Nat. Mater.* **10,** 429–433 (2011).

14. Wang, H. *et al.* Thermally Driven Large N-Type Voltage Responses from Hybrids of Carbon Nanotubes and Poly (3 , 4- ethylenedioxythiophene) with Tetrakis (dimethylamino) ethylene. *Adv. Mater.* **27,** 6855–6861 (2015).

15. Fan, Z., Du, D., Guan, X. & Ouyang, J. Nano Energy Polymer films with ultrahigh thermoelectric properties arising from significant seebeck coefficient enhancement by ion accumulation on surface. *Nano Energy* **51,** 481–488 (2018).

16. Hou, W. *et al.* Flexible Thermoelectric Cooling Devices. *Nano Energy* **50,** 766–776 (2018).

17. Finefrock, S., Zhu, X., Suna, Y. & Wu, Y. Flexible prototype thermoelectric devices based on Ag_2Te and PEDOT:PSS coated nylon fibre. *Nanoscale* **7,** 5598–5602 (2015).

18. Sun, C., Goharpey, A. H., Rai, A., Zhang, T. & Ko, D. Paper Thermoelectrics: Merging Nanotechnology with Naturally Abundant Fibrous Material. *ACS Appl. Mater. Interfaces* **8,** 22182–22189 (2016).

19. Rojas, J. P., Conchouso, D., Arevalo, A. & Singh, D. Nano Energy Paper-based origami flexible and foldable thermoelectric nanogenerator. *Nano Energy* **31,** 296–301 (2017).

20. Gao, J. *et al.* A novel glass- fiber-aided cold-press method for fabrication of n-type Ag_2Te nanowires. *J. Mater. Chem. A* **5,** 24740–24748 (2017).

21. Choi, J. *et al.* Large Voltage Generation of Flexible Thermoelectric Nanocrystal Thin Films by Finger Contact. *Adv. Energy Mater.* **7,** 1700972 (2017).

22. Jin, Q. *et al.* Cellulose Fiber-Based Hierarchical Porous Bismuth Telluride for High-Performance Flexible and Tailorable Thermoelectrics. *ACS Appl. Mater. Interfaces* **10,** 1743–1751 (2018).

23. Day, T. *et al.* Evaluating the potential for high thermoelectric efficiency of silver selenide. *J. Mater. Chem. C* **1,** 7568–7573 (2013).

24. Pei, J. *et al.* Rapid synthesis of Ag_2Se dendrites with enhanced electrical performance by microwave-assisted solution method. *New J. Chem.* **37,** 323–328 (2013).

25. Yang, D., Su, X., Meng, F., Wang, S. & Yan, Y. Facile room temperature solventless synthesis of high thermoelectric performance Ag_2Se via a dissociative adsorption reaction. *J. Mater. Chem. A* **5,** 23243–23251 (2017).

26. Ferhat, M. & Nagao, J. Thermoelectric and transport properties of β-Ag_2Se compounds. *J. Appl. Phys.* **88,** 813–816 (2000).

27. Perez-taborda, J. A., Caballero-calero, O., Vera-londono, L., Briones, F. & Martin-gonzalez, M. High Thermoelectric zT in n-Type Silver Selenide films at Room Temperature. *Adv. Energy Mater.* **8,** 1702024 (2018).

28. Chang, C. *et al.* 3D charge and 2D phonon transports leading to high out-of-plane ZT in n-type SnSe crystals. *Science* **360,** 778–783 (2018).

29. Liu, H. *et al.* Copper ion liquid-like thermoelectrics. *Nat. Mater.* **11,** 422–425 (2012).

30. Mu, X. *et al.* Enhanced electrical properties of stoichiometric $Bi_{0.5}Sb_{1.5}Te_3$ film with high-crystallinity via layer-by-layer in-situ Growth. *Nano Energy* **33,** 55–64 (2017).

31. Shi, X. *et al.* Room-temperature ductile inorganic semiconductor. *Nat. Mater.* **17,** (2018).

32. Song, H. *et al.* Polymer / carbon nanotube composite materials for flexible thermoelectric power generator. *Compos. Sci. Technol.* **153,** 71–83 (2017).

33. He, R., Schierning, G. & Nielsch, K. Thermoelectric Devices : A Review of Devices , Architectures , and Contact Optimization. *Adv. Mater. Technol.* **3,** 1700256 (2018).

34. Wang, L. *et al.* Solution-printable fullerene/TiS_2 organic/ inorganic hybrids for high-performance flexible n-type thermoelectrics. *Energy Environ. Sci.* **11,** 1307–1317 (2018).

35. Wan, C. *et al.* Flexible n-type thermoelectric materials by organic intercalation of layered transition metal dichalcogenide TiS_2. *Nat. Mater.* **14,** 622–627 (2015).

36. Liu, L. *et al.* Flexible unipolar thermoelectric devices based on patterned poly [K_x(Ni-ethylenetetrathiolate)] thin films. *Mater. Chem. Front.* **1,** 2111–2116 (2017).

37. Dun, C. *et al.* Flexible n-type thermoelectric films based on Cu-doped Bi_2Se_3 nanoplate and Polyvinylidene Fluoride composite with decoupled Seebeck coeffi cient and electrical conductivity. *Nano Energy* **18,** 306–314 (2015).

38. Chen, Y. *et al.* Bendable n-Type Metallic Nanocomposites with Large Thermoelectric Power Factor. *Adv. Mater.* **29,** 1604752 (2017).

39. Wan, C. *et al.* Ultrahigh thermoelectric power factor in flexible hybrid inorganic-organic superlattice. *Nat. Commun.* **8,** 1024 (2017).

40. Wei, Q. *et al.* Measurement of in-plane thermal conductivity in polymer films Measurement of in-plane thermal conductivity in polymer films. *AIP Adv.* **6,** 45315 (2016).

41. King, J. A., Tucker, K. W., Vogt, B. D., Weber, E. H. & Quan, C. Electrically and Thermally Conductive Nylon 6,6. *Polym. Compos.* **20,** 643–654 (1999).

42. Fang, C. M., Groot, R. A. De & Wiegers, G. A. Ab initio band structure calculations of the low-temperature phases. *J. Phys. Chem. solid* **63,** 457–464 (2002).

Acknowledgements

This work was supported by the Key Program of National Natural Science Foundation of china (5163210), National Basic Research Program of China (973 Program) under Grant No. 2013CB632500, the foundation of the State Key Lab of Advanced Technology for Material Synthesis and Processing (Wuhan University of Technology and the Technology), and Innovation Commission of Shenzhen Municipality (Grant Nos. KQTD20160226195659 91and KQCX20150331101823 70).

Author Contributions

Y.D. and K. C. conceived the idea, discussed and analyzed the data. Y. D. performed the majority of experiments and drafted the manuscript; K. C. designed the whole work and revised the manuscript; Y. Q and J. H. prepared the TEM sample and analyzed the microstructure by STEM; Q. Y. and L. C. contributed the thermoelectric properties measurement; L. C. proposed valuable advice for revising the manuscript. S. C. contributed the theoretical calculation. All authors discussed the results and commented on the manuscript.

Competing interests. The authors declare that there is no conflict of interests regarding the publication of this article